Inverse Problems in Radiative Transfer: Determination of Atmospheric Parameters

MOUSTAFA T. CHAHINE[1]

Jet Propulsion Laboratory, California Institute of Technology, Pasadena

(Manuscript received 9 February 1970, in revised form 12 June 1970)

ABSTRACT

It is shown that the relaxation method for inverse solution of the full radiative transfer equation leads to unique temperature profiles. Apart from its attractive simplicity, the algorithm is also capable of discriminating between noise and valid information without any need for data smoothing. A set of new inverse problems is formulated for the determination of the concentration of absorbing gases in an atmosphere, the extent and height of clouds, and surface elevations. The proposed methods are illustrated by examples in the earth's atmosphere for the region of the 4.3 μ CO_2 band.

1. Introduction

Inversion problems arise when the structure of a physical system is to be identified on the basis of observations of its output. The earth's atmosphere forms such a system suitable for study. Kaplan (1959) has suggested an observational technique to determine the vertical thermal structure of an atmosphere from measurements of the emerging specific intensity as a function of frequency, within appropriately selected spectral regions. A general algorithm for solving this problem by relaxation was developed (Chahine, 1968) and applied for independent determination of atmospheric temperature profiles without any *a priori* knowledge of the forms of the expected solutions.

The present paper discusses the problems of uniqueness and stability associated with the relaxation method of solution and in the presence of errors in the observations. As a consequence of the high stability of this nonlinear method, we formulate a new set of inverse problems for the determination of other important atmospheric characteristics connected with the internal atmospheric radiative flux, such as the concentration of absorbing gases, cloud top height, fractional cloud cover and surface elevations.

In the illustrations discussed in the text, the initial guess is taken to be an isothermal temperature profile at 200K unless otherwise stated.

2. Theoretical basis

The steady-state radiative transfer equation (RTE) for a plane parallel homogeneous atmosphere in local thermodynamic equilibrium appears as a set of linear, first-order, ordinary differential equations, one for each frequency. The form of the fundamental RTE appropriate to our purposes is

$$\frac{\cos\theta}{\rho(z)k(\nu)}\frac{dI(\nu,z,\theta)}{dz}=B[\nu,T(z)]-I(\nu,z,\theta), \qquad (1)$$

where I is the monochromatic radiance at frequency ν and in a direction forming an angle θ with the local vertical z, the mass absorption coefficient is $k(\nu)$, and $\rho(z)$ is the density of the absorbing gas. The source function B is given by the Planck blackbody function as

$$B[\nu,T(z)]=a\nu^3/(e^{b\nu/T}-1), \qquad (2)$$

where $T(z)$ is the temperature at height z.

It is convenient to transform the vertical height z to pressure p through the hydrostatic equation

$$\rho(z)dz=(-w/g)dp, \qquad (3)$$

where w is the mass mixing ratio of the absorbing gas and g is the gravitational acceleration, and to define

$$\tau(\nu,p)=\exp\left[\frac{w}{g}\int_{p}^{\bar{p}}k(\nu,p')dp'\right] \qquad (4)$$

as the transmittance by a column of absorbers between levels p and $\bar{p}$.

The intensity of the vertically outgoing monochromatic radiance arriving in a small solid angle (so that $\theta\approx 0$) at a pressure level $\bar{p}$ and frequency ν is obtained by direct solution of Eq. (1), subject to a blackbody boundary condition at the surface p_0, and is given by

$$I(\nu,\bar{p})=B[\nu,T(p_0)]\tau(\nu,p_0)+\int_{\ln p_0}^{\ln\bar{p}}B[\nu,T(p)]\frac{\partial\tau}{\partial(\ln p)}d(\ln p), \qquad (5a)$$

[1] On sabbatical at the Department of Meteorology, Massachusetts Institute of Technology.

in which $\partial\tau/\partial(\ln p)$ may be considered a weighting function. The surface emissivity is assumed here to be unity.

The requirement of finite spectral resolution, however, necessitates carrying out a frequency integration of Eq. (5a) over an interval $[\nu_1,\nu_2]$ to yield

$$I(\nu,\bar{p})=\int_{\nu_1}^{\nu_2}\phi(\nu,\nu')\left[B[\nu',T(p_0)]\tau(\nu',p_0)+\int_{\ln p_0}^{\ln\bar{p}}B[\nu',T(p)]\frac{\partial\tau}{\partial(\ln p)}d(\ln p)\right]d\nu', \quad (5b)$$

where $\phi(\nu,\nu')$ is the instrumental slit function.

The direct problem is relatively simple. It consists of the integral operation given in Eqs. (5) which transforms the variation of temperature with height into a variation of the emerging radiance with frequency. But despite the simplicity of the direct problem, the inverse problem turns out to be a difficult task (Kondratyev, 1969). Part of the difficulty in reconstructing the temperature profile from the radiance is associated with the fact that integral equations like (5), with fixed limits, *may not always* have a solution for an arbitrary function $I(\nu,\bar{p})$. Since the values of $I(\nu,\bar{p})$ are obtained from measurements which are only approximate, the reduction of this problem to a linear system is mathematically improper, and a nonlinear approach to the solution of the full equations becomes necessary.

The extraction of $T(p)$ from under the integration signs of Eqs. (5) is possible because, for certain frequency ranges, the transmittance τ between any pressure level and the measuring instrument depends heavily on frequency and altitude, i.e., the integrand of Eq. (5a) reaches a strong maximum at different heights according to the frequency. As a consequence of the mean-value theorem, the change in the outgoing radiance for one frequency ν_j and the change in the Planck function at one pressure level p_j can be related by

$$\frac{I(\nu_j,\bar{p})-(B\tau)_0}{I'(\nu_j,\bar{p})-(B\tau)_0'}=\frac{B[\nu_j,T(p_j)](\partial\tau/\partial\ln p)_{p_j}\Delta_j\ln p}{B[\nu_j,T'(p_j)](\partial\tau'/\partial\ln p)_{p_j}\Delta'_j\ln p}, \quad (6)$$

where T and T' are two different temperature profiles, and p_j is selected as the level at which the contribution of the integrand of Eq. (5a) to $I(\nu_j,\bar{p})$ is maximum or substantial. We define

$$\Delta_j\ln p=\frac{I(\nu_j,\bar{p})-B[\nu_j,T(p_0)]\tau(\nu_j,p_0)}{B[\nu_j,T(p_j)](\partial\tau/\partial\ln p)_{p_j}} \quad (7)$$

as the effective width of the weighting functions.

Because for certain frequencies with high attenuation, $\Delta_j\ln p$ remains small in comparison with the corresponding dimension of the active thickness of the atmosphere, and because the dependence of the Planck function on temperature variations is much stronger than that of $\partial\tau/\partial(\ln p)$, Eq. (6) can be approximated by

$$\frac{I(\nu_j,\bar{p})-(B\tau)_0}{I'(\nu_j,\bar{p})-(B\tau)_0'}\approx\frac{B[\nu_j,T(p_j)]}{B[\nu_j,T'(p_j)]}. \quad (8)$$

When the contribution to the outgoing radiance of the term $(B\tau)_0$ is dominant or negligible, we obtain the relaxation equation

$$\frac{I(\nu_j,\bar{p})}{I'(\nu_j,\bar{p})}\approx\frac{B[\nu_j,T(p_j)]}{B[\nu_j,T'(p_j)]}. \quad (9)$$

Since most of the vertically emerging radiance at the strongly absorbing frequencies arises from the upper regions of the atmosphere, and since that of the less attenuating frequencies comes from progressively lower levels, it is possible to select a set of frequencies to sound the atmosphere at different pressure levels. The size of a set of sounding frequencies is defined by the degree of vertical resolution required and is limited by the capabilities of the measuring instrument. The population of a set of sounding frequencies is not unique.

3. Iterative method of solution

Let us assume that measurements of the outgoing radiance $I(\nu_j,\bar{p})$ are available at a discrete set of J sounding frequencies and that the composition of the atmosphere, the instrumental slit function $\phi(\nu,\nu')$, and the detector level $\bar{p}$ are known. We can now proceed as follows to determine the corresponding temperature profile $T^{(n)}(p)$, where n is the order of iterations:

1) Make an initial guess, $n=0$ for $T^{(n)}(p_j)$. The initial guess can be almost any function, constant or otherwise.

2) Substitute $T^{(n)}(p_j)$ into Eqs. (5) and, using an accurate quadrature formula, evaluate the corresponding values of the outgoing radiance $I^{(n)}(\nu_j,\bar{p})$ for the given set of sounding frequencies.

3) Compare the computed radiance values $I^{(n)}(\nu_j,\bar{p})$ with the measured data $\tilde{I}(\nu_j,\bar{p})$. If the residuals

$$R_j^{(n)}=\frac{|\tilde{I}_j-I_j|}{\tilde{I}_j}, \quad (10)$$

approach zero for the individual sounding frequencies, or in an rms sense, $\langle R^{(n)}\rangle_{rms}$, then $T^{(n)}(p_j)$ is a solution.

4) If the residuals are different from zero, we apply the relaxation equation J times to generate a new guess for the corresponding values of temperature $T^{(n+1)}(p_j)$ at the selected J pressure levels. From Eqs. (2) and (9) the relaxation equation takes the form

$$T_j^{(n+1)}=\frac{b\nu_j}{\ln\{1-[1-\exp(b\nu_j/T_j^{(n)})](I_j^{(n)}/\tilde{I}_j)\}}. \quad (11)$$

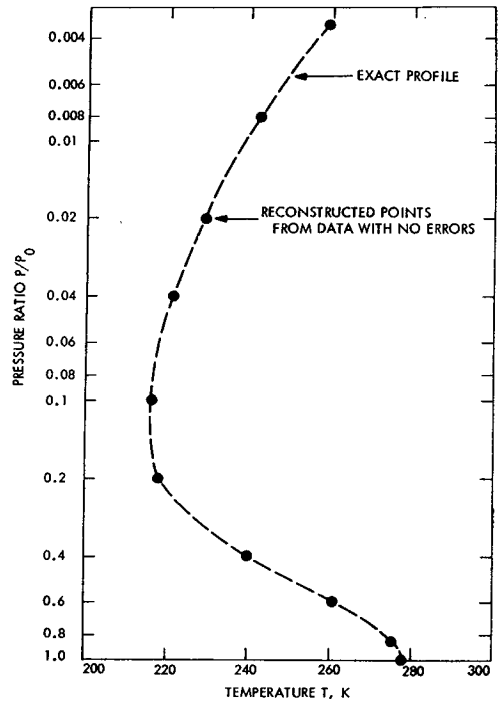

FIG. 1. Comparison between the exact temperature profile and the reconstructed temperature values for synthetic data with no errors.

In this operation, each sounding frequency ν_j acts at one specific pressure level p_j to relax $T^{(n)}(p_j)$ to $T^{(n+1)}(p_j)$.

5) With this new set of temperature values, go back to step 2) and repeat until the residuals approach zero.

4. Uniqueness of solutions

The relaxation method of solution has been applied to invert synthetic radiance data generated by a computer from a set of model temperature profiles in an atmosphere having a constant CO_2 mixing ratio of 462×10^{-6} by mass. The spectral interval selected to illustrate this study corresponds to the 33 frequencies, 2195 (5) 2355 cm^{-1}. The transmittance subroutine used (Gray and McClatchey, 1964) gives values of $\tau(\nu,p)$ at intervals of frequency equal to 5 cm^{-1} in the 4.3 μ CO_2 band. The instrumental slit function $\phi(\nu,\nu')$ is taken to be triangular, symmetrical with respect to ν, and having a base width equal to 40 cm^{-1}. A typical example of the accuracy of the reconstructed temperature values is shown in Fig. 1.

The typical results of Fig. 1 show two interesting properties which call for comment. First of all, examination of the solutions obtained by using as an initial guess any one of the isothermal profiles at 200, 250 and 300K, or the U. S. Standard Atmosphere temperature profiles, shows that all the reconstructed temperature values reproduced very well the original profile in less than seven iterations and the average absolute error in the reconstructed temperature, $\langle\Delta T\rangle_{av}$, is less than 0.1K, irrespective of the initial guess. Secondly, when a small perturbation of the order of 1K was superimposed on the exact profile and the resulting profile used as an initial guess, the solution converged with similar rapidity. The value of $\langle\Delta T\rangle_{av}$ decreased from 1K to 0.074K in one iteration only. These results show clearly that the final answers do not depend on the initial guess and that convergence is guaranteed for large as well as small perturbation solutions. Typically, 3 sec are required on the IBM 7094 to compute the temperature values shown in Fig. 1.

To pursue further the question of uniqueness, we studied the dependence of the solutions on the population of different sets of sounding frequencies. Some of the more salient features of the results are described here.

First, when we repeated the case of Fig. 1 using different sets of sounding frequencies, all in the 4.3 μ CO_2 band, we observed that the corresponding results showed no significant change in the final answer. In fact, the size of the solid circle in Fig. 1 is large enough to envelop the whole family of solutions resulting from seven sets of 10, three sets of 22, and one set of 33 sounding frequencies.

Secondly, we noticed that the residuals $R_j^{(n)}$ of the individual sounding frequencies do not converge simultaneously at the same order n of iteration. The reason for this is that in any given frequency range the absorption properties of the atmosphere do not allow for the selection of a uniform set of sounding frequencies for which the corresponding radiance values, $I(\nu_j,\bar{p})$, have equal information content with respect to their assigned pressure levels p_j. Therefore, the effect of higher order iterations tends to improve the solution corresponding to the relatively inefficient sounding frequencies, i.e., those for which convergence of $R_j^{(n)}$ is lagging, at the expense of accumulating truncation errors at the other sounding frequencies. In this circumstance it may be useful to allow the inefficient frequencies to continue their relaxation while inhibiting further the sounding frequencies which have already converged. Ideally, the selection of sounding frequencies jointly from several appropriate frequency ranges should provide a more efficient set.

As a consequence of this efficiency criterion, the vertical resolution of small details in a profile cannot be determined for a single pressure layer to the exclusion of the rest of the profile. The temperature values obtained according to the present algorithm show that the power of resolution is limited by the size of the set of sounding frequencies, their individual information content, and the effective widths of the weighting functions. This leads us to adopt the following inversion principle: *Any temperature variation related to observable variations in the emerging radiance can be reconstructed.*

5. Stability of solutions

The fact that the present iterative process converges to a given limit does not of itself imply that the result in a practical, remote sensing experiment will approach this limit. The present relaxation method of solution is necessarily a discrete numerical process in which the concept of formal convergence plays hardly any role, although it is involved in the analytical arguments by which the process is established. Therefore, our conclusions concerning stability and convergence should be judged according to the extent to which the present algorithm suppresses the effect of quadrature, random, and systematic errors on the final temperature profile. In the present work the rate of convergence will be judged by the rate with which the residuals $R_j^{(n)}$ of Eq. (10) approach their asymptotic values.

a. Quadrature errors

The effect of quadrature errors on the final answer depends on two sources: one of these is computational, resulting from the integrations of Eqs. (5) for the evaluation of $I^{(n)}(\nu_j,\bar{p})$; the other is due to interpolations resulting from the inability of a discrete set of points to fit the whole temperature profile exactly even for perfect answers. In the results typified by Fig. 1, a modified Simpson's rule was used to evaluate Eqs. (5) with a first-order interpolation formula for the intermediate values of temperature. The temperature profile in Fig. 1 is relatively smooth, and the use of a different interpolation formula or a larger number of sounding frequencies for such profiles is not warranted.

b. Random errors

The question of the propagation of random errors is a critical one and depends on a number of factors, including the spectral region in which the observations are made. In examining the tolerance of this algorithm to random errors, the effect of their distribution, their maximum values, and their rms values will be taken into consideration.

To obtain a feeling for the stability of the solution, errors were produced by a uniform random error generator subroutine; then they were added to the exact synthetic data, and inversions were performed for a variety of cases as in the previous section. In the results shown in Fig. 2, a set of 10 random errors having a maximum value of 9.3% and a rms value of 4.8% was superimposed on the exact synthetic data of Fig. 1. The reconstructed temperature values show an excellent tolerance to random errors. The average absolute error $\langle\Delta T\rangle_{av}$ in the temperature here is 1.5K.

Since the present inversion scheme is nonlinear, the effects of random errors must be examined for each case separately. The results of some 30 cases studied are summarized in Fig. 3. They show that, in observations made in the 4.3 μ region, a temperature accuracy $\langle\Delta T\rangle_{av}$ of 1K can be expected with a 2% rms random error in observations, and an accuracy of 2–3K can be expected with a 5–7% rms error in observations.

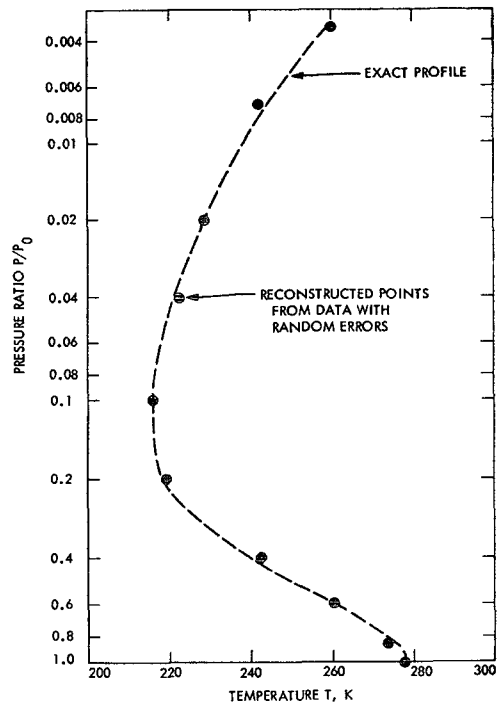

FIG. 2. Same as Fig. 1 except for synthetic data with random errors having a maximum value of 9.3% and an rms value of 4.8%.

The effects of random errors in observations vary according to the frequency and can be estimated in principle from Eqs. (2) and (5a). We consider a hypothetical set of sounding frequencies for which the weighting functions form a perfect set of delta functions. The dependence of errors in the temperature solution on random errors can be obtained by differentiation of the blackbody function with respect to temperature, to yield

$$\Delta T=\left[\frac{T^2(1-e^{-b\nu/T})}{b\nu}\right]\frac{\Delta B}{B}. \tag{12}$$

Eq. (12) shows that a relative error $\Delta B/B$ in measuring the blackbody radiance will be multiplied, by the ex-

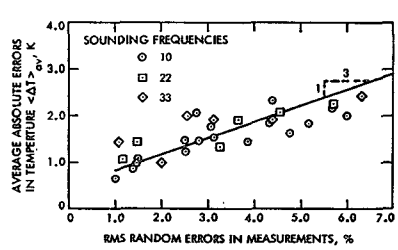

FIG. 3. Effect on the accuracy of the reconstructed temperature values of random errors in data, together with the least-squares-fitted straight line.

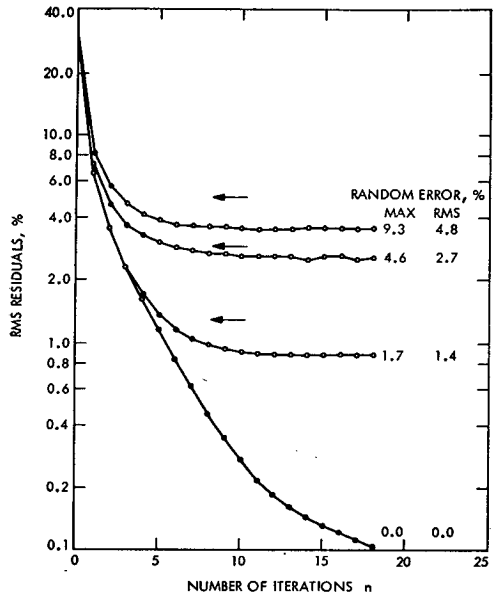

FIG. 4. Variation of the rms residuals with respect to the number of iterations and the initial random error. Horizontal arrows indicates the level of the rms values of random error in data. The initial guess is a U. S. Standard Atmosphere temperature profile. See text for discussion of the meaning of the open as compared to the solid circles.

pression between brackets, when the radiance is inverted to temperature. This ideal multiplication factor is a function of frequency. A comparison of this factor with the slope of the least-squares-fit line in Fig. 3 turns out to be very satisfactory.

Perhaps more significant is the effect of random errors in measurements on the behavior of the residuals $R_j^{(n)}$ of Eq. (10). In the case of Fig. 1 for zero random errors in observations, we recall that the solution converged after a small number of iterations. The variations of the corresponding rms value of the residuals, $\langle R^{(n)}\rangle_{\text{rms}}$, with respect to the order of iteration, is shown as the lowest curve in Fig. 4. By contrast, the uppermost curve corresponds to the case of Fig. 2, with an rms random error of 4.8%.

A closer examination of the various results shown in Fig. 4 reveals that the residuals tend toward different asymptotic values according to the values of the corresponding random errors in observations. For zero random errors, the asymptotic value is equal to the quadrature errors.

Thus, in the presence of random errors in measurements the residuals do not give a false indication of convergence; they will not tend toward zero. The residuals first decrease and then approach an asymptotic value of the same order of magnitude as the errors in measurements. This property is the result of the partial (nonlinear) dependence of several sounding frequencies on temperature variations at one pressure level, and suggests that the iterative process should be terminated when $\langle R^{(n)}\rangle_{\text{rms}}$ becomes equal to the value of rms errors in measurements. The effect of continued iterations beyond this point does not increase the amount of information extracted from the radiance observations; it simply increases the rate of accumulation of computational errors in the reconstructed temperature values.

The solid circles in Fig. 4 correspond to the terminal orders of iteration at which the average absolute error in the reconstructed temperature values $\langle \Delta T\rangle_{\text{av}}$ is within ± 0.1K of the minimum. The solid circles occur always in the region of maximum curvature of the variation of $\langle R^{(n)}\rangle_{\text{rms}}$ with respect to n.

Finally, we have observed that the propagation of an error arising from one sounding frequency appears to be weak and limited mainly to the corresponding pressure level. This property strongly suggests the existence of a correlation between the functions $I(\nu,\bar{p})$ and $T(p)$, and requires that the set of sounding frequencies be also representative of the variations of $I(\nu,\bar{p})$ with respect to ν.

c. *Systematic errors*

Certain transmittance errors resulting from an approximate knowledge of the composition and properties of the atmosphere are systematic errors. The effect of these errors on the behavior of the residuals is qualitatively similar to the effect of random errors; that is to say, the larger the error in transmittance, the larger the corresponding asymptotic value of the residuals. And inversely, the residuals tend to their minimum value when the errors in transmittance are minimum. We show next that by investigating the consequences of adopting the criterion which we shall call minimization of the residuals, we can develop a satisfactory method for the determination of several other meteorological parameters.

6. Determination of other atmospheric parameters

a. *Concentration of absorbing gases*

The emergent intensity is a function of w, the ratio of the mass of an absorbing gas to that of the whole atmosphere. Thus, for a given transmission law, w can be determined by the principle of minimizing the residuals. According to this principle, we seek by iteration the value of w which renders the residuals minimum, assuming the concentration of the other active gases to be known.

As an illustration, we applied this method to the synthetic data of Fig. 1, assuming, however, the value of w (which is equal to 462×10^{-6}) to be unknown. The results in Fig. 5 of the twelfth iteration clearly show that the residuals have one minimum at the correct value of the mixing ratio. The results of the third iteration, for which $T(p)$ is far from having converged, show that a good approximation to the value of the mixing ratio can be obtained with just a rough knowledge of the temperature profile.

The profile $q(p)$ of a non-uniformly mixed gas can be determined by iteration using the relaxation equation

$$\frac{\tilde{I}(\nu_j,\bar{p})}{I^{(n)}(\nu_j,\bar{p})}\approx\frac{\Delta\tau[\nu_j,p_j,q^{(n+1)}(p_j),\cdots]}{\Delta\tau[\nu_j,p_j,q^{(n)}(p_j),\cdots]}.$$

The above equations should be solved numerically to determine $q^{(n+1)}(p_j)$.

Since τ is a *functional* of $q(p)$, the properties of the resulting solution will be different from those discussed in this paper for $T(p)$ and should be studied separately. A detailed treatment of this problem will be discussed in a forthcoming paper.

b. *Extent and height of clouds*

The presence of clouds in a fraction N of the field of view of an instrument modifies the mean absorption properties of the atmosphere within the narrow solid angle of observations. The effect of these clouds depends on their thermodynamic properties and is a function of their height p_c. Eq. (5a) does not account for the presence of clouds; the transmittance is computed for a clear field of view. Thus, inverse solutions of Eqs. (5) for radiance observations in the presence of clouds should not converge to the correct temperature profile. The results shown in Fig. 6 are for a numerical experiment in which the synthetic radiance data were generated on a computer for values of N equal to 0.0 (0.20) 1.0 and for a single layer of clouds behaving like a blackbody in equilibrium with the local ambient temperature at $p_c=400$ mb. The apparent temperature profiles resulting from the inverse solution of Eqs. (5), in which τ was evaluated once for the U. S. Standard Atmosphere temperature profile, show different temperature values below the clouds corresponding to the different values of N. However, as a consequence of the high attenuation of the integrand of Eq. (5a), the reconstructed temperature values above p_c remain almost unaffected by the presence of the clouds. At the cloud level p_c this results in a difference of $\sim$1K in the value of $T(p_c)$. Thus, the cloud top height p_c can be deduced

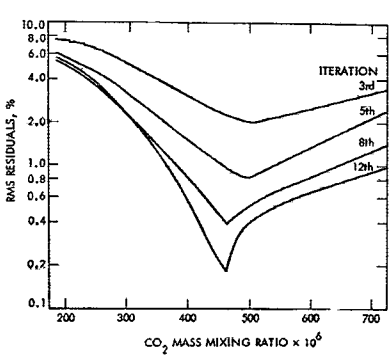

FIG. 5. Determination of the mass mixing ratio of an absorbing gas in an atmosphere by the criterion of minimization of the residuals.

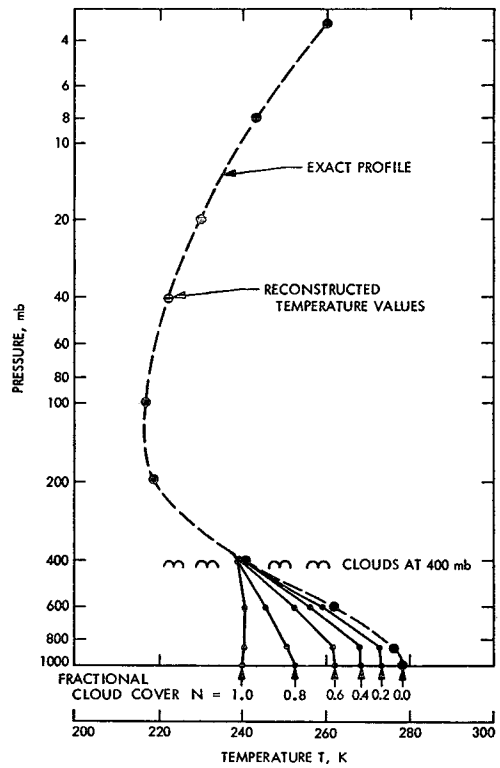

FIG. 6. Comparison between the exact temperature profile and the reconstructed apparent-temperature values according to Eqs. (5) in the presence of clouds.

either from one set of radiance measurements and a knowledge of the cloud top temperature T_c, or from two sets of radiance measurements made over two adjacent surface areas having different cloud covers in their respective fields of view.

The definition of the fractional cloud cover N is obtained from the RTE for a partly cloudy atmosphere. If we consider a single isothermal cloud layer acting like a blackbody at the local ambient temperature with emissivity $\epsilon_c=1$, then

$$I(\nu,\bar{p})=(1-N)\left[(B\tau)_0+\int_{\ln p_0}^{\ln\bar{p}}B\frac{\partial\tau}{\partial(\ln p)}d(\ln p)\right]+N\left[(B\tau)_c+\int_{\ln p_c}^{\ln\bar{p}}B\frac{\partial\tau}{\partial(\ln p)}d(\ln p)\right]. \quad (13)$$

We group terms on the right-hand side of Eq. (13), conform with the instrumental slit function according to Eq. (5b), and write

$$\tilde{I}(\nu,\bar{p})=I^{\text{clear}}(\nu,\bar{p})-NG(\nu,p_c). \quad (14)$$

Eq. (14) states that the measured radiance is equal to the value that would be received had the field of view been completely clear minus the radiance obscured by the presence of the clouds. The expression of N is defined by selecting a cloud-dependent frequency, say

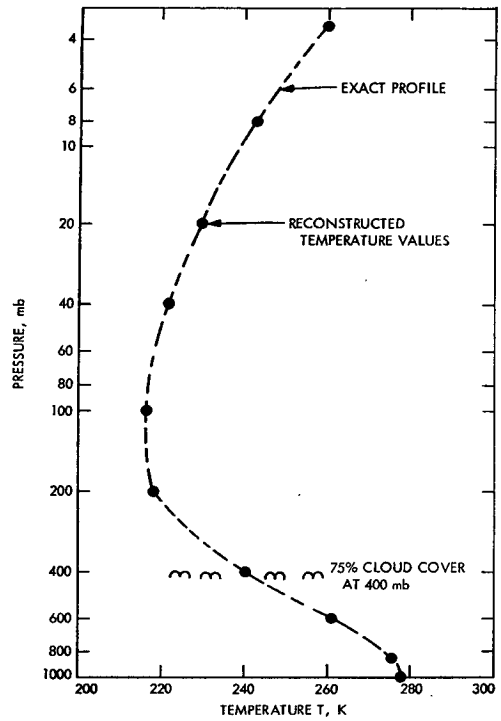

FIG. 7. Comparison between the exact temperature profile and the the reconstructed temperature values according to Eqs. (10)–(12) in the presence of a fractional cloud cover.

ν_i, having a substantial radiance contribution from the lower level of the atmosphere. If $\tilde{I}_i$ is the measured intensity at such a frequency, it follows from Eq. (14) that

$$N=\frac{I_i^{\text{clear}}-\tilde{I}_i}{G_i}. \tag{15}$$

Eq. (15) gives N as a functional transform of the unknown temperature profile.

After substituting (15) into (13), we find that the corresponding residuals $R_j^{(n)}$ defined by Eq. (10) are quite small for all the cloud-dependent frequencies and for any temperature profile under the clouds. Thus, in order to determine accurately the value of N and obtain a unique solution of the temperature profile under the clouds, it is necessary to have an extra parameter such as the value of the temperature at any level below the clouds, say $T(p_0)$ at the ground.

We conclude, therefore, that a knowledge of any one of the parameter combinations (p_c,N), (p_c,T_0), (T_c,N) or (T_c,T_0) is sufficient for the determination of the whole temperature profile in the clear portion of the field of view.

Fig. 7 shows the results of a hypothetical example for $N=75\%$ and $p_c=400$ mb. The synthetic radiance data, for the same set of sounding frequencies as in Fig. 1, were generated on a computer. The inverse solution of Eq. (13) was obtained by the relaxation method, assuming the combination (T_c,T_0) is known, with $T_c=242$K and $T_0=278$K. The reconstructed temperature values enjoy the same stable properties as for clear field of view. The reconstructed values of the fractional cloud cover and cloud top height were obtained by iteration; the results were $N=0.756$ and $p_c=395$ mb. The corresponding error in the reconstructed temperature profiles $\langle\Delta T\rangle_{\text{av}}$ is similar to that for the case of Fig. 1.

When the combination of two sets of radiances measured in adjacent fields of view and a knowledge of $T(p_0)$ is used to determine the temperature profile, the solutions for N, p_c and $T(p)$ should be carried out simultaneously. The underlying assumption here is that the radiances per unit area emerging from the clear portions of the two adjacent fields of view have the same value for the same sounding frequency. The value of p_c which minimizes the residuals corresponds to the cloud height.

c. Surface elevation

Land masses are not transparent to thermal radiation in the 4.3 and 15 μ regions. Thus, since no information can be received from below the surface, the reconstructed temperature profile is always isothermal below the surface level. In the 4.3 μ region, and for an instrumental slit function of 40 cm^{-1}, the high vertical temperature resolution permits surface elevations to be determined to within 25–50 mb in a cloudless atmosphere.

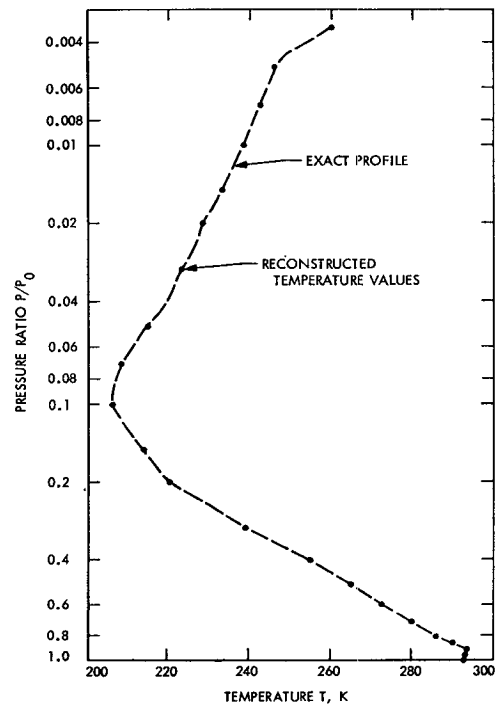

FIG. 8. Comparison between the exact temperature profile and the reconstructed temperature values. Observe the high vertical resolution obtained from 22 sounding frequencies with an instrumental slit function having a base width of 40 cm^{-1} in the 4.3 μ region.

Certain types of clouds are also opaque to thermal radiation, and in the case of a full overcast the inferred temperature profile will be isothermal below the cloud top as shown in Fig. 6 for the case of $N=1$.

7. Conclusion

Exact numerical solutions of the RTE are obtained for the determination of the temperature profile and other atmospheric parameters. The graphical illustrations presented in the text could have been made for inversions of a set of 22 or 33 sounding frequencies (see Fig. 8) without affecting any of the derived conclusions. The present algorithm is capable of making maximum use of the information available in the observations; therefore, it is desirable to apply this method jointly in the 15 and 4.3 μ CO_2 bands and in the microwave region.

Apart from these applications, the method is of intrinsic interest in that it provides much needed insight into the internal structure of the radiative transfer equation and consequently should aid in the proper design of remote sounding experiments. Perhaps of equal importance, the present algorithm furnishes a valuable check on the accuracy of other data reduction schemes, and defines the limits of the information that can be determined by remote soundings.

In a related test, the present method was successfully applied to reduce experimental radiance data measured during a balloon flight of a 4.3 μ CO_2 band grating spectrometer. The agreement between the reconstructed and radiosonde measured temperature profiles was excellent under various meteorological conditions, including partial cloudiness. Discussion of these results, however, falls outside the intended scope of this paper and is the subject of a separate study (Shaw *et al.*, 1970).

Acknowledgments. This paper presents the results of one phase of research carried out at the Department of Meteorology, Massachusetts Institute of Technology, and the Jet Propulsion Laboratory, California Institute of Technology, under Contract No. NAS 7–100, sponsored by the National Aeronautics and Space Administration.

REFERENCES

Chahine, M. T., 1968: Determination of the temperature profile in an atmosphere from its outgoing radiance. *J. Opt. Soc. Amer.*, **58**, 1634–1637.

Gray, L. D., and R. A. McClatchey, 1964: Atmospheric radiation: 4.2 to 5.0 microns. *Appl. Opt.*, **4**, 1624–1631.

Kaplan, L. D., 1959: Inference of atmospheric structure from remote radiation measurements. *J. Opt. Soc. Amer.*, **49**, 1004–1007.

Kondratyev, K. Ya., 1969: *Radiation in the Atmosphere.* New York, Academic Press, 624–654.

Shaw, J. H., M. T. Chahine, C. B. Farmer, L. D. Kaplan, R. A. McClatchey and P. W. Schaper, 1970: Atmospheric and surface properties from spectral radiance observations in the 4.3-micron region. *J. Atmos. Sci.*, **27**, 773–780.